EPJ Photovoltaics **14**, 26 (2023)

https://doi.org/10.1051/epjpv/2023017

Available online at:
www.epj-pv.org

Special Issue on 'Recent Advances in Photovoltaics 2022' edited by Mohamed Amara, Thomas Fix, Jean-Paul Kleider, Judikaël Le Rouzo and Denis Mencaraglia

REGULAR ARTICLE OPEN ACCESS

A multicriteria analysis of the potential degradations of a photovoltaic module to assess its robustness

Islem Boujlel[1,2], Pierre-Olivier Logerais[2,*], Rached Ben Younes[1], Mahamadou Abdou Tankari[2], and Abdellatif Bouaichi[3]

[1] Université de Gafsa, TEMI, Faculté des Sciences, 2112 Gafsa, Tunisia
[2] Univ. Paris-Est Créteil, CERTES, 61 avenue du Général de Gaulle, 94010 Créteil, France
[3] SMARTiLab, EMSI Rabat, avenue Oqba, angle rue Assouhaili, 10000 Rabat, Morocco

Received: 1 March 2023 / Received in final form: 4 June 2023 / Accepted: 19 July 2023

Abstract. Photovoltaic (PV) modules in service undergo more or less severe degradation depending on their operating environments, ages and technologies. In this work, we investigated the coupled influence of the climatic conditions of operation and of the degree of deterioration of a PV module on its energy production. We considered four silicon PV modules characterized in standard test conditions. The PV conversion is modeled by a single diode model taking into account the presence of a fault. Matlab/Simulink software was used to calculate the energy supplied at a constant load for the PV module with and without defects. The ratio between the energy produced with fault and without fault allowed to quantify the percentage of loss. This loss was plotted according to the degrees of degradation of the short-circuit current I_{sc}, the open-circuit voltage V_{oc}, the series resistance R_s and the shunt resistance R_{sh}. It is shown that when irradiance is held constant, the energy loss is lower with increasing temperature for I_{sc} and R_{sh}, and vice versa for V_{oc} and R_s. While the temperature is kept constant, the energy loss is lower when the irradiance increases for I_{sc} and R_{sh}, and inversely for V_{oc} and R_s. A multicriteria analysis enabled to determine the most robust module among the four ones.

Keywords: Photovoltaic module / degradation / temperature / irradiance / simulation / multicriteria analysis

1 Introduction

Solar photovoltaic (PV) energy is the most widely used of the renewable energy sources [1]. It consists in converting the electromagnetic radiation from the sun into electricity by means of solar cells that are expected to function in a variety of different environments [2,3]. The operating of solar cells depends strongly on internal parameters related to the device itself and to the technology of elaboration of the photovoltaic device, and also on external ones linked to the conditions of usage. The global irradiance, the temperature and the wind speed are indeed important factors that govern the behavior and the performance of solar cells [4]. Additionally, natural aging causes the emergence of degradations such as corrosion, delamination, discoloration, cracks and glass breakage, hot spots and PID (Potential-Induced Degradation) within the PV modules [2,5], impacting the efficiency and reliability of the PV systems. For these reasons, it is necessary to adapt the design of PV modules to delay the occurrence of defects for as long as possible. In practice, PV module degradations can be identified in situ by measuring alterations of their current−voltage ($I-V$) curves translated in standard test conditions (STC) and by matching them with the specific fault signature of the defects. Furthermore, simulation is an attractive tool to explore the production behavior of a PV module [6]. It enables, for example, to indicate the power reduction regarding the environmental and climatic conditions of use for a degraded PV module [7]. The choice of suitable PV technologies is driven by material, economic and environmental criteria. In this regard, a multicriteria approach can be implemented for the decision-making based on the sorting and selection or ranking of the different options chosen for the PV panels [8–10].

In the present study, the issue of the degree of degradation of a PV module and its coupling with climatic parameters is addressed. Our objective is to investigate the robustness of a PV module before its use in a given environment, knowing only the specifications of its datasheet in standard test conditions (STC). A modeling approach followed by a multicriteria analysis is proposed. Simulation results for four PV modules are compared for a set of irradiances and temperatures.

The paper is organized as follows. In the first part, we recall the degradation modes of silicon PV modules and

* e-mail: pierre-olivier.logerais@u-pec.fr

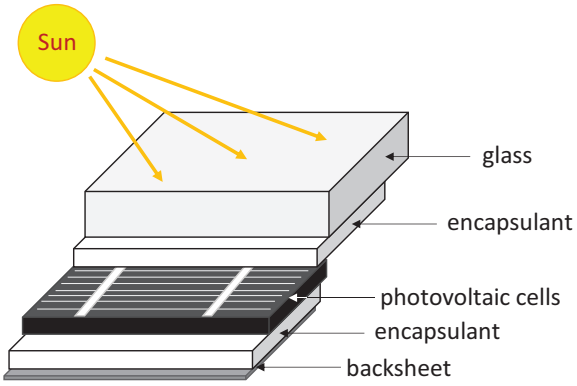

Fig. 1. The various components of a photovoltaic module subjected to degradation.

their signatures on the *I*–*V* characteristics. The second part deals with the model used and the method to simulate the real production of a PV module in the presence of a degraded parameter associated with a defect. The third part is intended for the presentation and the discussion of the obtained results. At last, a general conclusion and some perspectives are given.

2 Material and method

2.1. Degradation of photovoltaic modules and impact on the *I*–*V* characteristics

The performance of photovoltaic modules under field conditions can be reduced by several factors such as temperature, humidity, irradiance, dust and mechanical shocks. Natural aging induces a gradual deterioration of the characteristics of a photovoltaic module that eventually impairs its ability to operate within the acceptability criteria [5]. The degraded state of the photovoltaic module can become problematic when the degradation exceeds a critical threshold. Indeed, photovoltaic module manufacturers consider a photovoltaic module to be faulty when its efficiency reaches a level below 80% of its initial value.

The outdoor exposure of a photovoltaic module can affect its different parts which are recalled in Figure 1 [11]. Also, these degradations can be encountered for accelerated tests [12,13]. Six classes of effects on the current-voltage (*I*–*V*) characteristic are defined in the report "Review of Failures of Photovoltaic Modules" [5] which provides the main degradation mechanisms associated with effects on the *I*–*V* curve.

– *Class no. 1: Degradation of the short-circuit current* I_{sc} – The short-circuit current becomes lower than expected, such as when reducing the incident irradiance, in the case of a loss of transparency due to browning or yellowing of the encapsulant [14], corrosion of the glass reducing light trapping [15] or delamination causing optical decoupling of the layers [16]. The shape of the $I-V$ characteristic changes whether the deteriorations are homogeneous or heterogeneous.
– *Class no. 2: Degradation of the open-circuit voltage* V_{oc} – The open-circuit voltage is reduced by faulty cell interconnections [17] and with light-induced degradation (LID) of crystalline silicon modules or in the presence of potential-induced degradation (PID).
– *Class no. 3: Degradation of the series resistance* R_s – The series resistance becomes higher when there is an increase in the interconnect resistance and in the presence of corrosion in the junction box [18].
– *Class no. 4: Degradation of the shunt resistance* R_{sh} – The $I-V$ curve in the vicinity of the short-circuit current I_{sc} becomes more inclined, which means that the shunt resistance is decreased due to heterogeneous transparency loss [19] or in the presence of heterogeneous corrosion in the anti-reflection coating of the PV cells [20].
– Class no. 5: *Slope change at the vicinity of the maximum power point* P_{max} – A deviation of the slope at the point of maximum power can be caused by several anomalies such as degradation of the interconnections, corrosion of the soldering joints and of the junction box [20] or in the presence of a defective reverse-biased diode.
– *Class no. 6: Effect of shading* – A "staircase" shape is obtained for the current-voltage curve under partial shading of the PV module forcing the current to flow through a shunt diode, lowering at the same time the generated voltage and the maximum power. Consequently, in an array of PV modules arranged in series/parallel, the presence of a single shaded module can affect the overall power output [20].

2.2 Studied system and methodology

The studied system is that of a PV module, with and without defect, supplying its produced power to a fixed load of resistance R_m (in Ω) so as to operate at maximum power point at STC conditions [21] (Fig. 2):

$$R_m = \frac{V_m}{I_m} \tag{1}$$

where V_m is the maximum voltage (in V) and I_m is the maximum current (in A) in STC conditions for the non-defective PV module. Both V_m and I_m are usually provided by the manufacturer in the datasheet of commercial PV modules. This system is configured as a standalone application.

2.3 Methodology

The presence of a fault causes a decline in the *I*–*V* characteristic of the PV module. We consider here the degradations belonging to classes 1 to 4 encountered for natural aging or after accelerated tests previously described in Section 2.1. These alterations have an impact on the parameters I_{sc}, V_{oc}, R_s and R_{sh}. Each of these parameters, designed by X, is degraded by a degree D which can be expressed in percentage:

$$D(\%) = \frac{X}{X_{ref}} \tag{2}$$

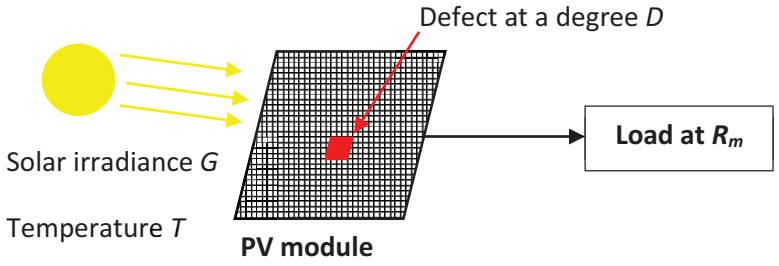

Fig. 2. Configuration of the studied PV system.

where X_{ref} corresponds to the value of I_{sc}, V_{oc}, R_s or R_{sh} under STC given by the manufacturer of the non-defective PV module.

The instantaneous power output $P(t)$ of the PV module (in W) is given by:

$$P(t) = V(t).I(t) \tag{3}$$

where V and I are the voltage (in V) and the current (in A) respectively, and t represents the time (in s).

By integrating this power over a day, from sunrise to sunset, the energy supplied to the load during a day E_{day} (in J) is obtained:

$$E_{day} = \int_0^{day} P(t).dt. \tag{4}$$

The normalized energy E_{loss} (in %) is defined as the ratio between the energy produced by the PV module in the presence of a degree D degradation to that without degradation for the same input conditions and load R_m:

$$E_{loss} = \frac{E_{day,\,with\ degradation\ of\ degree\ D}}{E_{day,\,without\ any\ degradation}}. \tag{5}$$

The value of D giving an energy loss of 20% for a parameter X, is called D^*. The latter is found by means of a fitting curve (Fig. 3). Once determined, the values of D^* are reported in a table for all the parameters X. We have considered a reduction of 20% which is inspired by that of the warranty of the manufacturers of PV modules who guarantee a power higher than 80% of the initial power after 25 years of use.

To quantify the overall degree impact of the degradation taking into account the four X parameters for one given module, the following sum is calculated [8]:

$$sum = \sum_{i=1}^{4} \alpha_i D^*(X) \tag{6}$$

where α_i is the weight of each parameter X. When comparing several PV modules, the calculated sums can be confronted in order to determine the most robust PV module introducing the same input conditions.

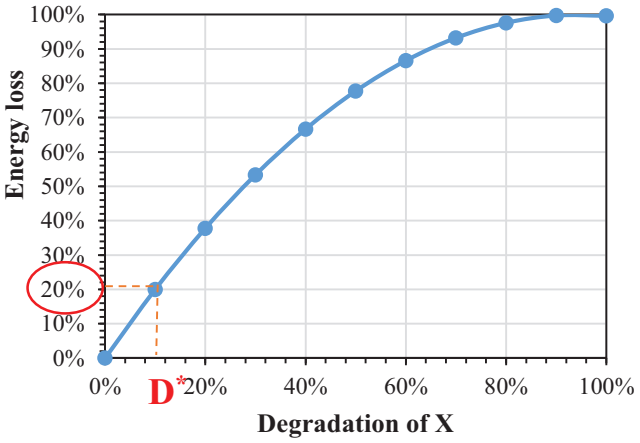

Fig. 3. Curve of the effect of irradiance and temperature on the energy loss as a function of degradation of an X parameter for a PV module.

3 Modeling and simulation

We used the one-diode-equivalent electrical circuit of a photovoltaic module (Fig. 4). The circuit consists of a current source, a diode in parallel, a shunt resistance R_{sh} which represents the leakage resistance between the two areas n and p of the junction, and a series resistance R_s which represents the internal resistance through which the electric current I flows. We employed the five-parameter model established by Villalva et al. which puts to use an iterative Newton−Raphson algorithm to calculate the values of the series and shunt resistances by adjusting the $I-V$ curve to fit the experimental maximum power provided in the datasheet of the PV module [22]. The interest in using this model lies in its numerical accuracy, especially for high irradiances, and in its ease of handling [22–25]. Its global accuracy was estimated at ±2.24% taking two cases of silicon PV modules [23].

In this approach, the current I and voltage V for a photovoltaic module that contains N_s cells in series are related by [22]:

$$I = I_{pv} - I_0\left[exp\left(\frac{V + R_s.I}{V_t.a}\right) - 1\right] - \frac{V + R_s.I}{R_{sh}} \tag{7}$$

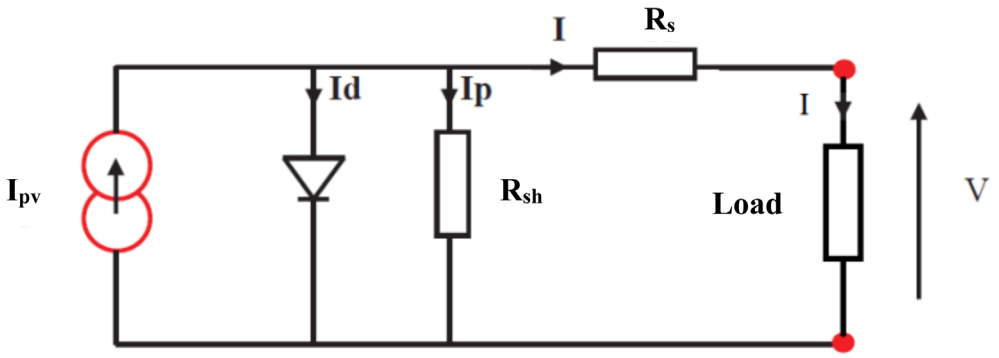

Fig. 4. Equivalent circuit of a photovoltaic module.

in which V_t is the thermal voltage:

$$V_t = \frac{N_s.k.T}{q} \tag{8}$$

where $q = 1.60217646 \times 10^{-19}$ C is the electron charge (1.6×10^{-19} C), $k = 1.38 \times 10^{-23}$ J.K^{-1} is the Boltzmann constant, T is the junction temperature (in K), and N_s is the number of cells connected in series; I_{pv} is the current generated by the incident light directly proportional to the solar irradiance G [26,27]:

$$I_{pv} = \left(I_{pv,n} + K_I \Delta T\right) \frac{G}{G_n} \tag{9}$$

where $I_{pv,n}$ is the current generated by the incident light under an irradiance $G_n = 1000$ W.m^{-2}, K_I is the current temperature coefficient (in A.K^{-1}), $T = T - T_n$ is the temperature difference with $T_n = 25\,^\circ$C; I_0 is the saturation current [26,27]:

$$I_0 = \frac{I_{sc,n} + K_I \Delta T}{exp\frac{\left(V_{oc,n} + K_V T\right)}{a.V_t} - 1} \tag{10}$$

where $I_{sc,n}$ and $V_{oc,n}$ are the values of the short-circuit current (in A) and the open-circuit voltage (in V) under STC conditions, K_V is the voltage temperature coefficient (in V . K $^{-1}$), and a is the ideality factor. It can be noted that I_{pv} and I_0 are temperature dependent [22,26,27].

Calculations were performed using a tool named SOPHEE (standing for Solar PV Energy Estimation) realized with the Matlab language and involving a "Matlab GUI" interface [28]. The interface is displayed in Figure 5. The values provided in the datasheet of one PV module are entered in the interface with the value of the load and also the ones of the climatic parameters over a day (file with irradiance and temperature profiles). Equations (7)–(10) are solved accordingly using blocks interconnected by mathematical operators in the Simulink platform. The degraded input values can be introduced as well. The tool enables to display the evolution of the power calculated according to equation (3), the mean power and the energy supplied to the load by integrating the power following equation (4) with fitting curves. For our study, the calculated energies were then recorded on another file so as to calculate the energy loss according to equation (5). The SOPHEE tool can also be applied to simulate the degradation of the performance of a PV module according to the years of operating, introducing aging laws into the interface (see Fig. 5).

We considered for the simulations and comparisons three polycrystalline silicon modules (of types KC200GT, MSX60 and PW1560) and one monocrystalline silicon (of type Q6LM) having well-detailed datasheets and for which the single diode model had been validated in previous studies. A good agreement between the single diode model results and the curves under STC was shown for irradiances between 400 W.m^{-2} and 1000 W.m^{-2} and cell temperatures between 25°C and 75 °C for these four PV modules [22]. The SOPHEE tool provided us with similar results for the initial cases (non-defective PV modules). The technical parameters necessary for the simulation of the four PV modules displayed in Table 1 were extracted from their datasheets. The values of the degradation levels D indicated in Table 2 for the four X parameters were entered. A 16-hour day is assumed for the calculations of the generated energies. For the input data, two sets of values were defined. First, the irradiance G was varied from 100 to 1000 W.m^{-2} with a step of 200 W.m^{-2} while considering a module temperature $T = 25\,^\circ$C. Second, the cell temperatures T were successively of 0 °C, 10 °C, 25 °C, 45 °C and 80 °C considering an irradiance at 1000 W.m^{-2}.

4 Results and discussion

The effect of the degradation of I_{sc}, V_{oc}, R_s and R_{sh} associated with the degradation modes of classes 1 to 4 are described here with regard to irradiance and temperature. Then, a multicriteria analysis is conducted and perspectives are given.

4.1 Effect of irradiance

Figure 6 displays for the four considered PV modules the normalized energy loss E_{loss} as a function of the degree of degradation D for I_{sc}, V_{oc}, R_s and R_{sh} in the case of the five irradiance values with a cell temperature at 25 °C.

Table 1. Technical parameters of the four photovoltaic modules in STC.

	KG200GT	Q6LM.m	MSX60	PW1650
Current at P_{max} (I_m) (A)	7.61	7.11	3.5	4.8
Voltage at P_{max} (V_m) (V)	26.3	0.5113	17.1	34.4
Short-circuit current I_{sc} (A)	8.21	7.6	3.8	5.1
Open-circuit voltage V_{oc} (V)	32.9	0.6118	21.1	43.2
No-load voltage/temperature coefficient K_V (V/K)	−0.1230	−0.0037	$-80\ 10^{-3}$	−0.158
Short circuit current/ temperature coefficient K_I (A/K)	0.0032	0.0005	0.003	0.00146
Number of cells connected in series N_s	54	1	36	72
Ideality factor a	1.3	1.2	1.3	1.0
Shunt resistance R_{sh} (Ω)	415.405	5.0001	304.833	2013.58
Series resistance R_s (Ω)	0.221	0.0012	0.2	0.72
Surface	1425 mm × 990 mm	156 mm× 156 mm	1105 mm× 502 mm	1237 mm × 1044 mm
Load R_m (Ω)	3.45	0.071	4.885	7.166

Table 2. Range of variations for the degrees of degradation.

Parameter X	Range of variation for D					Weight α_i
	Values				Relative percentages	
	KG200GT	Q6LM.m	MSX60	PW1650		
I_{sc}	[0 ; 8.21]	[0 ; 7.16]	[0 ; 3.8]	[0 ; 5.1]	[0 ; 100%]	1
V_{oc}	[0 ; 32.9]	[0 ; 0.6118]	[0 ; 21.1]	[0 ; 43.2]	[0 ; 100%]	1
R_s	[0.221 ; 2.43]	[0.0012 ; 0,12]	[0.2 ; 20.2]	[0.72 ; 72.72]	[100% ; 1000%]	0.1
R_{sh}	[0 ; 415.405]	[0.5 ; 5.0001]	[30.48 ; 304.83]	[201.36 ; 2013.581]	[0 ; 100%]	1

– *Class no. 1: Degradation of the short-circuit current I_{sc}* – It can be observed that, in the presence of degradation of I_{sc}, the energy loss in percentage is reduced when the irradiance augments. The difference in the energy loss is significant between 20 and 50% of degradation of I_{sc}. The discrepancy in the energy loss attains 20% between an irradiance of $100\,\mathrm{W.m^{-2}}$ and $1000\,\mathrm{W.m^{-2}}$. This difference is inferior to 5% when the degradation of I_{sc} exceeds 80%.

– *Class n° 2. Degradation of the open-circuit voltage V_{oc}* − A degradation threshold can be viewed for the energy loss which appears at higher degradation levels when the irradiance decreases. The threshold is at 50% degradation of the initial V_{oc} for an irradiance of $100\,\mathrm{W.m^{-2}}$, whereas for 800 and $1000\,\mathrm{W.m^{-2}}$, the degradation of V_{oc} increasingly affects the energy loss. There is a total energy loss when the degradation of V_{oc} is beyond 90%.

– *Class n° 3: Degradation of the series resistance R_s*– The energy loss becomes higher when R_s is more degraded and when the irradiance augments. Contrary to the first two cases, for I_{sc} and V_{oc}, where close behaviors between the four PV modules were found, it is interesting to note that the energy of the PV modules is differently affected by the relative degradation of R_s. When multiplied by ten and considering an irradiance of $1000\,\mathrm{W.m^{-2}}$, the relative energy loss is of 18% for the Q6LM.m PV module 68% for KC200GT and 70% for both PW1650 and MSX60. This means that the level of corrosion can have a different impact on the produced energy depending on the PV module.

– Class n° 4: *Degradation of the shunt resistance R_{sh}* − The change in R_{sh} has a limited effect on the energy. It is necessary to reach 80% of the degradation of R_{sh} to have a notable influence on the energy produced. The energy loss remains inferior to 15% for a degradation of R_{sh} above 80%.

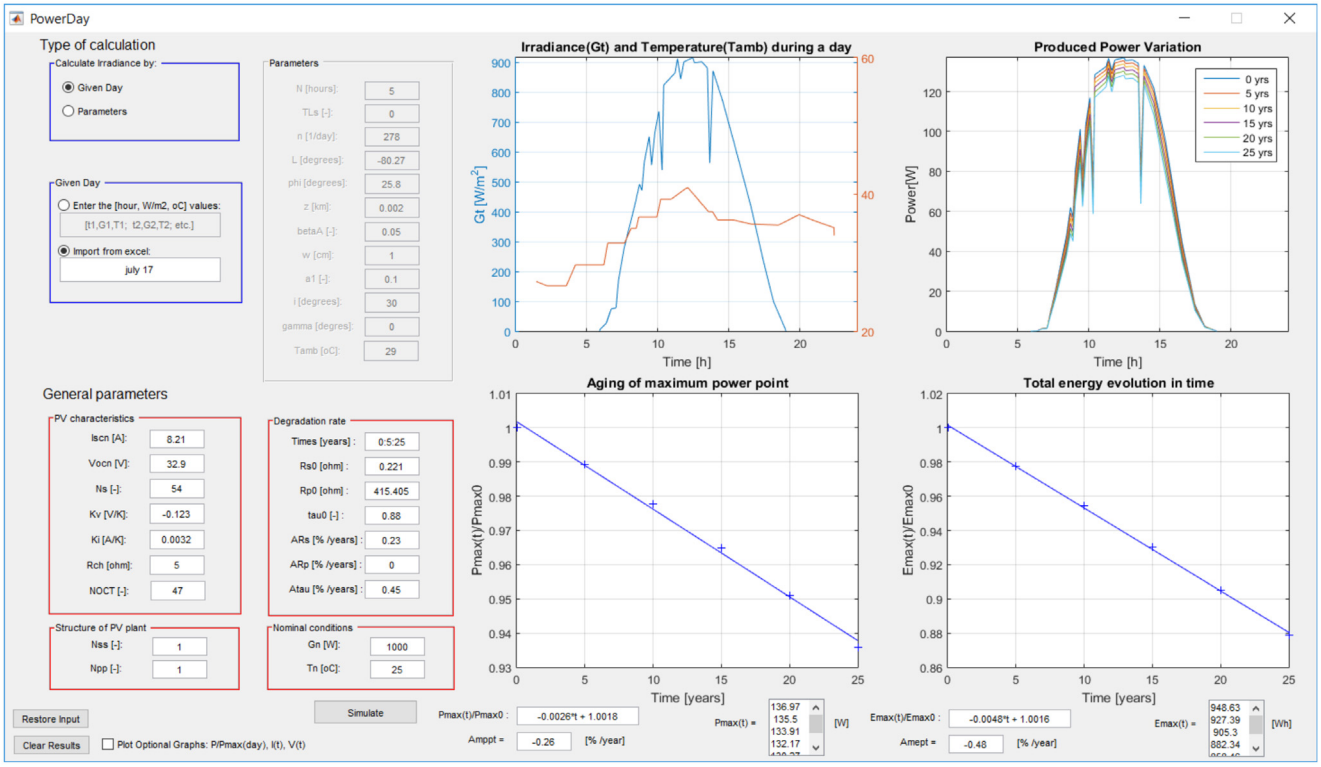

Fig. 5. The "Matlab GUI" interface called SOPHEE [28].

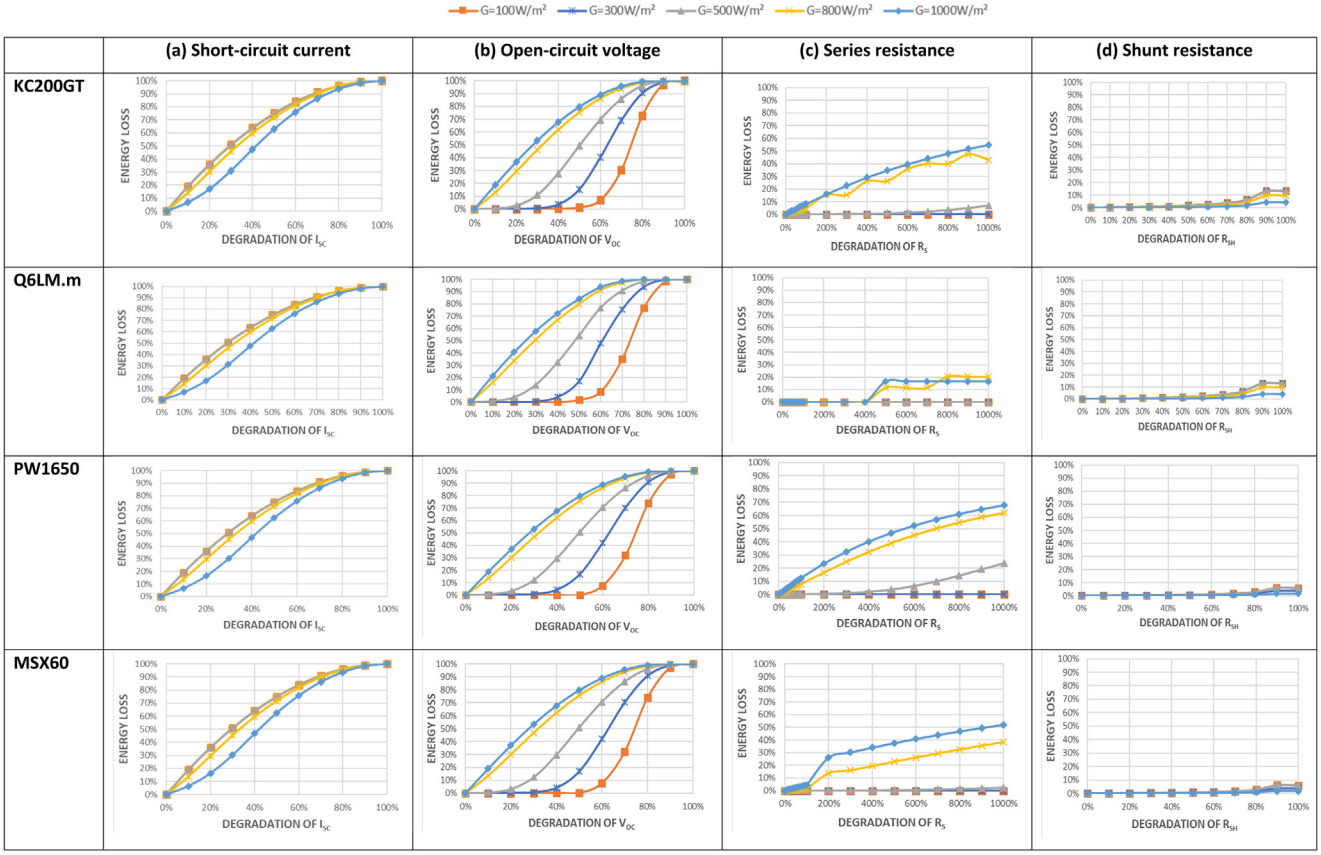

Fig. 6. Effect of irradiance on the energy loss as a function of the degradation of parameters I_{sc}, V_{oc}, R_s and R_{sh} at $T = 25\,°C$ (a) short-circuit current, (b) open-circuit voltage, (c) series resistance, and (d) shunt resistance for the four PV modules.

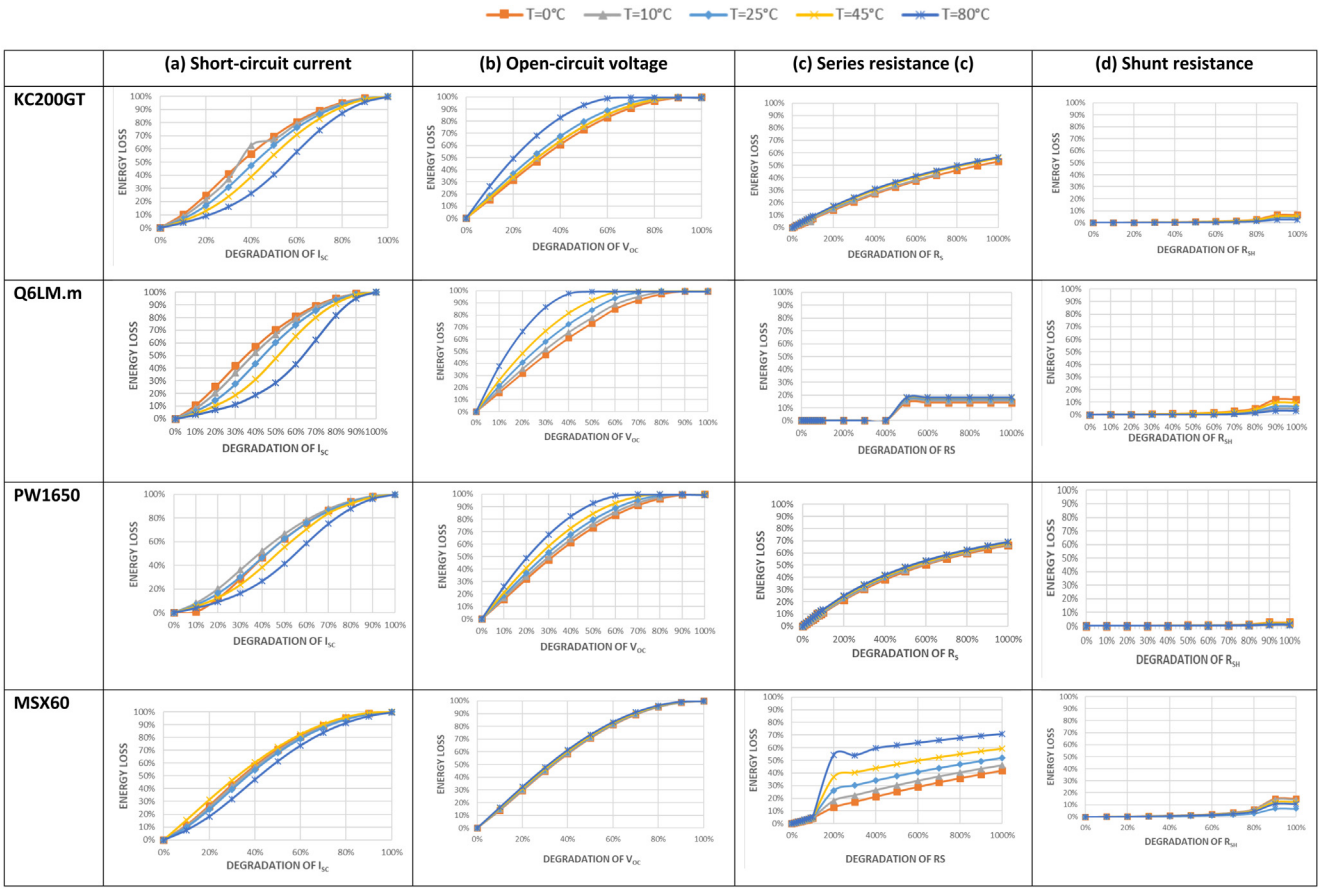

Fig. 7. Effect of temperature on the energy loss as a function of degradation of parameters I_{sc}, V_{oc}, R_s and R_{sh} at $G = 1000\,\mathrm{W.m^{-2}}$ (a) short-circuit current, (b) open-circuit voltage, (c) series resistance, and (d) shunt resistance for the four PV modules.

4.2 Effect of temperature

Figure 7 depicts the results found with a constant irradiance of $1000\,\mathrm{W.m^{-2}}$ for the different values of the module temperature ranging from 0 to 80 °C.

– *Class no. 1: Degradation of the short-circuit current* I_{sc} – The energy loss is higher in percentage as the module temperature diminishes. The variation in the percentage of energy loss is more pronounced for a degradation of I_{sc} between 20 and 80%, but the differences between the curves are not the same from one module to another. The variations in relative energy loss between a module with a temperature of 0 and 80 °C can be as high as 40% for the Q6LM.m PV module, 30% for the KC200GT, 25% for the PW1650 and 13% for the MSX60.

– *Class no. 2. Degradation of the open-circuit voltage* V_{oc} – The higher the temperature of the photovoltaic modules, all the more substantial is the energy loss. The energy loss curves are within a 5% difference for the MSX60 PV module, whereas the differences are more marked in the other three cases, particularly for the Q6LM.m PV module. An energy loss plateau of 100% is reached at 90% degradation of V_{oc} for the MSX60, 60% for the KC200GT and PW1650 PV modules, and 50% for the Q6LM.m PV module.

– *Class no. 3: Degradation of the series resistance* R_s – The energy loss in percentage increases with the temperature according to the degradation of the series resistance R_s, but in a different manner for the four PV modules. The evolutions are close to each other except for the PV module MSX60. The degradation of the PV modules KC200GT and PW1650 is increased from 0 to 55% and 68% respectively. Different behaviors can be noticed for the PV modules of types Q6LM.m and MSX60 having lower surfaces. Concerning the Q6LM.m PV module, upon applying five times the initial series resistance, there is no impact on the energy. There is a step with saturation at 15% beyond 500% R_s degradation. For the MSX60 PV module, the energy loss is more important with the degradation and the loss is higher for more elevated temperatures. The energy loss is of 70% for an increase of ten times in the series resistance.

– *Class no. 4: Degradation of the shunt resistance* R_{sh} – There is no energy loss below 80% degradation of R_{sh}. Above 80%, when the temperature is lower, the energy

Table 3. Values of D^* for the four PV modules varying the irradiance at a cell temperature of 25 °C.

Module KC200GT					
G (W.m^{-2})	$I_{sc}/I_{sc,ref}$	$V_{oc}/V_{oc,ref}$	$R_s/R_{s,ref}$	$R_{sh}/R_{sh,ref}$	**Sum**
100	10%	66%	1000%	100%	276%
300	10%	52%	1000%	100%	262%
500	10%	36%	1000%	100%	246%
800	10%	14%	350%	100%	159%
1000	22%	10%	260%	100%	158%
Sum for all the irradiances					1101%
Module PW1650					
G (W.m^{-2})	$I_{sc}/I_{sc,ref}$	$V_{oc}/V_{oc,ref}$	$R_s/R_{s,ref}$	$R_{sh}/R_{sh,ref}$	**Sum**
100	15%	63%	1000%	100%	278%
300	15%	48%	1000%	100%	263%
500	15%	38%	850%	100%	238%
800	17%	19%	220%	100%	158%
1000	22%	17%	180%	100%	157%
Sum for all the irradiances					1094%
Module MSX60					
G (W.m^{-2})	$I_{sc}/I_{sc,ref}$	$V_{oc}/V_{oc,ref}$	$R_s/R_{s,ref}$	$R_{sh}/R_{sh,ref}$	**Sum**
100	15%	63%	1000%	100%	232%
300	15%	48%	1000%	100%	234%
500	15%	38%	1000%	100%	253%
800	17%	19%	400%	100%	205%
1000	22%	17%	180%	100%	203%
Sum for all the irradiances					1127%
Module Q6LM.m					
G (W.m^{-2})	$I_{sc}/I_{sc,ref}$	$V_{oc}/V_{oc,ref}$	$R_s/R_{s,ref}$	$R_{sh}/R_{sh,ref}$	**Sum**
100	10%	68%	1000%	100%	278%
300	10%	52%	1000%	100%	262%
500	10%	34%	1000%	100%	244%
800	14%	12%	800%	100%	206%
1000	22%	10%	1000%	100%	232%
Sum for all the irradiances					1222%

loss is raised. With a temperature of 0 °C, the energy loss reaches 2% and 8% for the PW1650 and KC200GT PV modules which have higher surfaces, and 12% and 15% for the Q6LM.m and MSX60 PV modules with lower surfaces.

4.3. Multicriteria analysis

Tables 3 and 4 give the sums calculated with relation (6) accounting for all the four X degraded parameters with the considered irradiance and temperature values. The Q6LM.m module with the highest sum appears to be the most robust one for both the parametric simulations. For the irradiance variation at a cell temperature $T = 25$ °C, the global sum for the Q6LM.m PV module is 1222% against values around 1100% for the three other PV modules. The difference is more pronounced for the temperature variations at an irradiance of 1000 W.m^{-2}. The Q6LM.m PV module has a global sum of 1180% against values around 775% for the three other PV modules. Given these results, the Q6LM.m PV module would be more interesting to use as it seems less sensitive to the degradations and also to both the irradiance and the temperature. However, its surface and power are of 156 mm × 156 mm and 3.64 W making this PV panel solely interesting for low-power autonomous applications. On the other hand, the other three PV modules (KC200GT, PW1650, MSX60) have lower global sums, but nevertheless, deliver more elevated maximum power due to their larger

Table 4. Values of D^* for the four PV modules varying the cell temperature at an irradiance of $G = 1000\,\mathrm{W.m^{-2}}$.

Module KC200GT					
$\boldsymbol{T}$ (°C)	$\boldsymbol{I_{sc}/I_{sc,ref}}$	$\boldsymbol{V_{oc}/V_{oc,ref}}$	$\boldsymbol{R_s/R_{s,ref}}$	$\boldsymbol{R_{sh}/R_{sh,ref}}$	**Sum**
0	16%	16%	240%	100%	152%
10	20%	12%	240%	100%	156%
25	22%	12%	240%	100%	156%
45	26%	12%	220%	100%	160%
80	34%	8%	220%	100%	164%
Sum for all the temperatures					788%
Module PW1650					
$\boldsymbol{T}$ (°C)	$\boldsymbol{I_{sc}/I_{sc,ref}}$	$\boldsymbol{V_{oc}/V_{oc,ref}}$	$\boldsymbol{R_s/R_{s,ref}}$	$\boldsymbol{R_{sh}/R_{sh,ref}}$	**Sum**
0	24%	14%	400%	100%	178%
10	20%	12%	200%	100%	152%
25	22%	10%	180%	100%	150%
45	28%	10%	170%	100%	155%
80	34%	8%	160%	100%	158%
Sum for all the temperatures					793%
Module MSX60					
$\boldsymbol{T}$ (°C)	$\boldsymbol{I_{sc}/I_{sc,ref}}$	$\boldsymbol{V_{oc}/V_{oc,ref}}$	$\boldsymbol{R_s/R_{s,ref}}$	$\boldsymbol{R_{sh}/R_{sh,ref}}$	**Sum**
0	14%	15%	400%	100%	149%
10	14%	15%	200%	100%	149%
25	16%	15%	180%	100%	149%
45	12%	14%	170%	100%	143%
80	20%	13%	160%	100%	149%
Sum for all the temperatures					759%
Module Q6LM.m					
$\boldsymbol{T}$ (°C)	$\boldsymbol{I_{sc}/I_{sc,ref}}$	$\boldsymbol{V_{oc}/V_{oc,ref}}$	$\boldsymbol{R_s/R_{s,ref}}$	$\boldsymbol{R_{sh}/R_{sh,ref}}$	**Sum**
0	16%	14%	1000%	100%	230%
10	20%	12%	1000%	100%	232%
25	24%	10%	1000%	100%	234%
45	30%	8%	1000%	100%	238%
80	40%	6%	1000%	100%	246%
Sum for all the temperatures					1180%

surfaces. Thus, to optimize the robustness during the design phase of the PV modules, it would be interesting to use an inverse approach for sizing them consisting in increasing the global sum, and broadening if possible their surfaces, for the given climatic conditions of the place of utilization.

Also, it should be noticed that the level of degradation D^* varies in the same manner according to the irradiance and the temperature. It decreases for the short-circuit current I_{sc} and the resistance series R_s as the irradiance becomes more elevated and has an opposite behavior for the open-circuit voltage V_{oc}. The level of degradation D^* is never reached for the shunt resistance R_{sh}. Regarding the temperature, the behaviors are alike for the four PV modules: augmentation for the short-circuit current I_{sc} when the temperature becomes higher and the contrary for the open-circuit voltage V_{oc} and the series resistance R_s. The same remark can be made for the shunt resistance R_{sh}.

4.4. Perspectives

This study opens up the following perspectives. We used constant values for the irradiance and the temperature to show the effectiveness of the method, but the consideration of recorded climatic data to simulate real operating conditions is the next step as well as envisaging different PV systems at different scales. Here a standalone application with a constant load was targeted, but the methodology could be applied to a grid-connected system with maximum power point tracking.

The physical degradations impacting the I–V curves were specified in Section 2.1. This first investigation aimed at defining a methodology to quantify the impact of one level of degradation on the energy output of a PV module. Based on this approach, it will be possible to conduct specific studies involving one degradation mode (cracking, corrosion, soiling...), its structural properties, its level of degradation D and the associated lowering of the energy production, the reference case being the one without degradation.

We only took into consideration the degradation of effects belonging to classes 1 to 4. The effect of classes 5 and 6 could also be envisaged. To study them, it is not obvious to carry out parametric studies, and it will be necessary to rely on detailed case studies.

The modules were chosen according to the literature having well-detailed datasheets compared to other modules. The proposed method could be applied to higher-power modules, now being released. Finally, the sensibility of the simulation can certainly be improved for high irradiances by using a two-diode model taking into account with more exactness the resistive losses and the recombinations.

5 Conclusion

It is necessary to orient the choice of technical characteristics and technology of the PV modules in order to maintain a satisfactory level of performance throughout the life of the PV system despite the appearance of defects related to natural aging. A method to quantify the robustness of a PV module knowing the specifications of its manufacturer under standard test conditions (STC) was proposed. Four types of silicon PV modules were studied. The percentage of energy loss was plotted according to the degree of deterioration of the short-circuit current, the open-circuit voltage, the series resistance and the shunt resistance, given that they are individually associated with specific degradation modes. The level of the degradation giving 20% of loss regarding the initial energy produced was determined for each of the four parameters for a set of irradiances and a set of temperatures. The Q6LM.m PV module, having both a smaller surface and power, appeared to be the most robust one. It would indeed be interesting to use it for low-power applications. PV modules with larger surfaces and powers showed more sensitivity to degradation. By using the present approach, it would be worth raising the sum of the multicriteria analysis so as to optimize the choice of the materials and the sizes of PV modules prior to operating in a defined environment.

Different perspectives were provided. In the future, this approach can be implemented with weather data from different climates and with well-targeted degradation modes for an environment in order to determine the most suitable PV module for a given operating location. We have chosen here to decouple all the degradation effects in this first study, but a coupling of degradation effects could as well be something worth considering.

The authors are highly grateful to the University of Gafsa and to the Tunisian Ministry of Education and Research for funding this work. They would also like to extend their sincere thanks to Mrs. Wilhelmina Logerais, a native English speaker, for re-reading this paper.

Author contribution statement

Islem Boujlel carried out the calculations and the writing of this article. Pierre-Olivier Logerais supervised the work and participated in the elaboration and finalization of the paper. Rached Ben Younes, Mahamadou Abdou Tankari and Abdellatif Bouaichi contributed certain items to the contents.

References

1. J. Guzman-Henao, L.F. Grisales-Noreña, B.J. Restrepo-Cuestas, O.D. Danilo Montoya, Optimal integration of photovoltaic systems in distribution networks from a technical, financial, and environmental perspective, Energies **16**, 562 (2023)
2. M.A. Quintana, D.L. King, T.J. McMahon et al., Commonly observed degradation in field-aged photovoltaic modules, in *Conference Record of the Twenty-Ninth IEEE Photovoltaic Specialists Conference*, 2002, pp. 1436–1439
3. A. Bouaichi, A.A. Merrouni, C. Hajjaj, C. Messaoudi, A. Ghennioui, A. Benlarabi, H. Zitouni, In-situ evaluation of the early PV module degradation of various technologies under harsh climatic conditions: the case of Morocco, Renewable Energy **143**, 1500 (2019)
4. A. Al-Bashir, M. Al-Dweri, A. Al-Ghandoor, B. Hammad, W. Al-Kouz, Analysis of effects of solar irradiance, cell temperature and wind speed on photovoltaic systems performance, Int. J. Energy Econ. Policy **10**, 353 (2019)
5. M. Köntges, S. Kurtz, C. Packard, U. Jahn, K.A. Berger, K. Kato, T. Friesen, H. Liu, M.V. Iseghem, Review of Failures of PV Modules, Report IEA-PVPS T13–01:2014 (2014)
6. H. Yatimi, E. Aroudam, M. Louzazni, Modeling and simulation of photovoltaic module using MATLAB/SIMULINK, MATEC Web of Conferences **11**, 03018 (2014)
7. P.O. Logerais, O. Riou, R. Doumane M. Balistrou, J.F. Durastanti, Étude par simulation de l'influence du vieillissement et des conditions climatiques sur la production électrique d'un module photovoltaïque, in *16èmes Journées Internationales de Thermique, JITH 2013*
8. C. Zopounidis, P.M. Pardalos, *Handbook of multicriteria analysis* (Springer Science & Business Media, 2010)
9. N. Mukisa, R. Zamora, T. Lie, X. Wu, G, Chen, Multi criteria analysis ranking of solar photovoltaic modules manufacturing countries by an importing country, a case of Uganda, Solar Energy **223**, 326 (2021)
10. F. Balo, L. Sagbansua, The selection of the best solar panel for the photovoltaic system design by using AHP, Energy Procedia **100**, 50 (2016)
11. J.A. Tsanakas, L. Ha, C. Buerhop, Faults and infrared thermographic diagnosis in operating c-Si photovoltaic modules: A review of research and future challenges, Renew. Sust. Energy Rev. **62**, 695 (2016)

12. S. Spataru, P. Hacke, D. Sera, In-situ measurement of power loss for crystalline silicon modules undergoing thermal cycling and mechanical loading stress testing, Energies **14**, 72 (2021)
13. N.A. Ashtiani, S.M. Azizi, S.A. Khajehoddin, Robust control design for high-power density PV converters in weak grids, IEEE Trans. Controm Syst. Technol. **27**, 2361 (2018)
14. W. Luo, C.E. Clement, Y.S. Khoo, Y. Wang, A.M. Khaing, T. Reindl, A. Kumar, M. Pravettoni, Photovoltaic Module Failures after 10 Years of Operation in the Tropics, Renewable energy **177**, 327 (2021)
15. R. Ahrizi, W. Baouandji, M. Mostefaoui, L'influence du changement climatique sur les performances des modules photovoltaïques, thesis, Université Ahmed Draia-Adrar, 2017
16. G. Oreski, G.M. Wallner, Aging mechanisms of polymeric films for PV encapsulation, Sol. Energy, **79**, 612 (2005)
17. L. Bun, Détection et Localisation de Défauts pour un Système PV, thesis, Université de Grenoble, 2011
18. R. Khenfer, Détection et isolation de défauts combinant des méthodes à base de données appliquées aux systèmes électro-énergétiques, thesis, 2018
19. A. Benhalima, A. Djoubar, Étude comparative des modèles mathématiques explicites de caractérisation photovoltaique, thesis, University of Msila, 2021
20. A. Belaout, Étude et diagnostic des défauts fréquents aux systèmes photovoltaïques (PV) par emploi de la caractéristique courant-tension, thesis, 2018
21. D. Shmilovitz, On the control of photovoltaic maximum power point tracker via output parameters, IEE Proc. Electr. Power Appl. **152**, 239 (2005)
22. M.G. Villalva, J.R. Gazoli, E. Ruppert Filho, Modeling and circuit-based simulation of photovoltaic arrays, in *2009 Brazilian Power Electronics Conference,* (IEEE, 2009), pp. 1244–1254
23. A. Orioli, A. Di Gangi, A Criterion for Rating the Usability and Accuracy of the One-Diode Models for Photovoltaic Modules, Energies **9**, 427 (2016)
24. I. Drouiche, S. Harrouni, A. Hadj Arab, A new approach for modelling the aging PV module upon experimental I–V curves by combining translation method and five-parameters model, Electr. Power Syst. Res. **163**, 231 (2018)
25. K. Lappalainen, S. Valkealahti, Analysis of the operation of PV strings at the MPP closest to the nominal MPP voltage instead of the global MPP based on measured current-voltage curves, EPJ Photovoltaics **13**, 4 (2022)
26. G. Walker, Evaluating MPPT converter topologies using a Matlab PV model, J. Electr. Electron. Eng. Australia **21**, 49 (2001)
27. W. De Soto, S.A. Klein, W.A. Beckman, Improvement and validation of a model for photovoltaic array performance, Solar Energy **80**, 78 (2006)
28. C. Adrian, P.O. Logerais, Realizarea unei interfete matlab pentru modelarea grafică si numerică a efectului de imbătrânire a panourilor fotovoltaice, Master 2 report, June 2017

Cite this article as: Islem Boujlel, Pierre-Olivier Logerais, Rached Ben Younes, Mahamadou Abdou Tankari, Abdellatif Bouaichi, Bouaichi, A multicriteria analysis of the potential degradations of a photovoltaic module to assess its robustness, EPJ Photovoltaics **14**, 26 (2023)